Nonlinear Science and Intelligent Applications
https://www.acadlore.com/journals/NSIA

Modeling and Analysis of Inductively Coupled Identical Linear Resistive–Capacitive Shunted Josephson Junction Circuits

Alex Stephane Kemnang Tsafack[1,2*], Lucienne Makouo[3], Oumate Alhadji Abba[4], Noel Freddy Fotie Foka[5], Godpromesse Kenne[2]

[1] Research Unit of Condensed Matter of Electronics and Signal Processing, Department of Renewable Energy, Faculty of Science, University of Dschang, 67 Dschang, Cameroon
[2] Research Unit of Automation and Applied Computer (RU-AIA), Department of Electrical Engineering IUT-FV, University of Dschang, 134 Bandjoun, Cameroon
[3] Department of Civil Engineering and Architecture, National Higher Polytechnic Institute, University of Bamenda, 39 Bamenda, Cameroon
[4] Department of Physics, Faculty of Science, University of Maroua, 814 Maroua, Cameroon
[5] Department of Physics, Faculty of Science, University of Yaoundé I, 11584 Yaoundé, Cameroon

* Correspondence: Alex Stephane Kemnang Tsafack (alexstephanekemnang@gmail.com)

Received: 08-13-2025 **Revised:** 10-07-2025 **Accepted:** 10-16-2025

Citation: A. S. K. Tsafack, L. Makouo, O. A. Abba, N. F. F. Foka, and G. Kenne, "Modeling and analysis of inductively coupled identical linear resistive–capacitive shunted Josephson junction circuits," *Nonlinear Sci. Intell. Appl.*, vol. 1, no. 2, pp. 56–64, 2025. https://doi.org/10.56578/nsia010201.

Abstract: An inductively coupled system composed of two identical linear resistive-capacitive shunted Josephson junction (LRCSJJ) circuits driven by external direct current (DC) sources was modeled and analyzed in this study. The coupling between the junctions was realized through a shared inductor. The existence and nature of equilibrium states were shown to depend critically on the normalized DC bias currents applied to the junctions. It was demonstrated that the coupled LRCSJJ system admits either an unique equilibrium point or no equilibrium points at all, depending on the biasing conditions. A comprehensive linear stability analysis of the equilibrium point was carried out, revealing that its stability is jointly governed by the inductive coupling strength and the magnitude of the normalized DC currents. When a single stable equilibrium point exists, the system operates in an excitable regime. Conversely, when equilibrium points are absent, sustained oscillatory dynamics emerge. The analysis highlights the role of inductive coupling in regulating the balance between dissipation, energy storage, and nonlinear Josephson dynamics, thereby shaping the global behavior of the coupled system. These results provide fundamental insight into the controllable dynamical regimes of inductively coupled Josephson junction (JJ) circuits and may be of relevance for the design of superconducting electronic devices, including neuromorphic circuits and high-frequency oscillators, where excitability and oscillation play a functional role.

Keywords: Josephson junction; Inductive coupling; Stability analysis; Direct current bias; Excitable mode; Oscillatory mode

1 Introduction

A Josephson junction (JJ) is a superconducting device formed by two superconducting materials separated by an extremely thin insulating barrier, through which charge carriers are able to tunnel quantum mechanically [1, 2]. When no external voltage is applied, a supercurrent flows across the junction, commonly referred to as the Josephson current, and the associated charge transfer mechanism is known as Josephson tunneling [3]. This phenomenon, termed the Josephson effect, was theoretically predicted by Brian David Josephson and subsequently verified experimentally. Since its discovery, the Josephson effect has attracted considerable attention owing to its remarkable physical properties, wide range of potential technological applications, and the diversity of dynamical behaviors exhibited by JJ-based circuits [4–7]. The dynamics of JJs are strongly affected by external magnetic fields, and their exceptional sensitivity has made them fundamental components in advanced superconducting devices, including superconducting quantum interference devices and ultra-high-speed computing systems [1, 8].

Several theoretical models have been developed to describe JJ circuits, such as the linear resistive-capacitive shunted Josephson junction (LRCSJJ), the nonlinear resistive-capacitive shunted Josephson junction, the nonlinear resistive-capacitive inductive shunted Josephson junction, and the linear resistive-capacitive inductive shunted Josephson junction models [3–5, 9–12]. Previous investigations have shown that the nonlinear resistive-capacitive shunted Josephson junction and LRCSJJ circuits can exhibit chaotic dynamics when driven by external alternating current sources, whereas the linear resistive-capacitive inductive shunted Josephson junction and nonlinear resistive-capacitive inductive shunted Josephson junction configurations are capable of generating chaotic oscillations even under direct current (DC) excitation. From an engineering perspective, JJs powered by DC current sources are often preferred because of their structural simplicity, reduced power consumption, and practical implementation compared to alternating current-driven configurations [13–16]. Moreover, practical applications frequently require arrays or networks of JJs rather than isolated elements. Consequently, it is of critical importance to understand not only the behavior of a single JJ but also the collective dynamics arising from interactions between neighboring junctions [17, 18].

Coupling between JJs can be achieved through resistive, capacitive, or inductive elements. While the physical and dynamical properties of resistively coupled JJs have been extensively investigated [13, 17–23], comparatively fewer studies have focused on inductive or capacitive coupling mechanisms [24]. In particular, Agaoglou et al. [24] analyzed the nonlinear dynamics of two parametrically driven JJs coupled inductively via mutual inductance and reported the emergence of complex behaviors, including chaos. Recent studies have highlighted the complex dynamics of coupled JJ systems. Ngatcha et al. [25] reported transitions from incoherent states to coherent traveling waves in nonlocally coupled JJs driven by Wien bridge oscillators. Similarly, Metsebo et al. [26] showed that the equilibrium structure, stability, and birhythmic behavior of a resistive-capacitive shunted JJ coupled to a linear resistor-inductor-capacitor resonator strongly depend on the external DC source and system parameters.

Despite the significant progress made in the study of JJ-based circuits, several open issues remain regarding the analytical characterization of inductively coupled systems driven by DC sources. In particular, while nonlinear JJ models and alternating current-driven configurations have been widely investigated, the dynamical behavior of identical LRCSJJs coupled inductively under pure DC excitation has received comparatively little attention. Moreover, existing works often emphasize numerical observations, leaving a lack of systematic analytical insight into the equilibrium structure, stability conditions, and bifurcation mechanisms governing such systems. From both a fundamental and an engineering perspective, inductive coupling constitutes a physically realistic and non-dissipative interaction mechanism that naturally arises in superconducting circuits. Understanding how this coupling, in combination with external DC sources, influences the collective dynamics of JJs is therefore essential for the reliable design and control of superconducting devices exhibiting excitable or oscillatory responses.

Motivated by these considerations, the present work investigates a system of two identical LRCSJJ circuits coupled through an inductor and driven by independent DC current sources. The primary objective is to provide a comprehensive analytical and numerical study of the system, focusing on the existence and stability of equilibrium points, the role of the coupling strength and normalized DC currents, and the emergence of distinct dynamical regimes. In particular, the transition between excitable behavior and sustained oscillatory motion is examined in detail. By adopting the LRCSJJ framework, this study offers clear analytical tractability while capturing the essential physical mechanisms underlying the dynamics of inductively coupled JJs. The results contribute to a deeper understanding of coupled superconducting systems and lay the groundwork for future investigations of non-identical junctions and more complex dynamical phenomena.

The remainder of this study is organized as follows. Section 2 presents the formulation of the mathematical model and the analytical derivation of the governing equations for the inductively coupled LRCSJJ system. Section 3 is devoted to the numerical analysis and discussion of the system dynamics. Finally, the main findings are summarized in the concluding section.

2 Modeling and Analytical Analysis of Inductively Coupled Direct Current-Driven Identical Linear Resistive-Capacitive Shunted Josephson Junction Circuits

Figure 1 shows two identical LRCSJJ circuits which are connected to each other via a coupling inductor L.

The electrical circuit in Figure 1 consists of capacitors (C_1 and C_2), resistors (R_1 and R_2), an inductor (L), external DC driving sources ($I_{ex,1}$ and $I_{ex,2}$), and ideal JJ elements. The tunnel current $I_{JC,j}\sin(\phi_j)$ and the junction voltage $V_j = \frac{h}{4\pi e}\frac{\mathrm{d}\phi_j}{\mathrm{dt}}$ (j = 1, 2) can be obtained from the Josephson phases ϕ_j(t), where h is the Planck constant and e is the elementary charge. The inductively coupled LRCSJJ model in Figure 1 are identical; thus, $R_1 = R_2 = R$, $C_1 = C_2 = C$, and $I_{cj,1} = I_{cj,2} = I_{cj}$. Applying Kirchhoff's current law at nodes A and B yields the following equations:

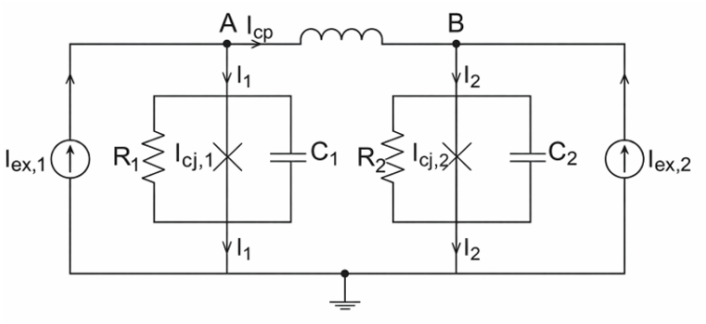

Figure 1. Electrical circuit of inductively coupled direct current (DC)-driven linear resistive-capacitive shunted Josephson junction (LRCSJJ) circuits

$$\begin{aligned} I_{\mathrm{ex},1} &= \frac{hC_1}{4\pi e}\frac{\mathrm{d}^2\phi_1}{\mathrm{d}t'^2} + \frac{h}{4\pi R_1}\frac{\mathrm{d}\phi_1}{\mathrm{d}t'} + I_{JC}\sin(\phi_1) + I_{cp} \\ I_{\mathrm{ex},2} &= \frac{hC_2}{4\pi e}\frac{\mathrm{d}^2\phi_2}{\mathrm{d}t'^2} + \frac{h}{4\pi R_{1,2}}\frac{\mathrm{d}\phi_2}{\mathrm{d}t'} + I_{JC}\sin(\phi_2) - I_{cp} \end{aligned} \tag{1}$$

The voltage across the inductor is given by:

$$V_L = V_A - V_B \Rightarrow -L\frac{\mathrm{d}I_{cp}}{\mathrm{d}t'} = \frac{h}{4\pi e}\left(\frac{\mathrm{d}\phi_1}{\mathrm{d}t'} - \frac{\mathrm{d}\phi_2}{\mathrm{d}t'}\right) \tag{2}$$

Solving Eq. (2) yields the following equation:

$$I_{cp} = \frac{h}{4\pi eL}(\phi_2 - \phi_1) \tag{3}$$

Substituting Eq. (2) in System (1) yields the dimensionless rate equations:

$$\begin{aligned} \frac{\mathrm{d}^2\phi_1}{\mathrm{d}t'^2} + \alpha\frac{\mathrm{d}\phi_1}{\mathrm{d}t'} + \sin(\phi_1) &= i_1 + \varepsilon(\phi_1 - \phi_2) \\ \frac{\mathrm{d}^2\phi_2}{\mathrm{d}t'^2} + \alpha\frac{\mathrm{d}\phi_2}{\mathrm{d}t'} + \sin(\phi_2) &= i_2 + \varepsilon(\phi_2 - \phi_1) \end{aligned} \tag{4}$$

where, $\Omega = \left[\frac{(4\pi eI_{JC})}{(hC)}\right]^{\frac{1}{2}}$, $t = \Omega t'$, $\alpha = 1/(RC\Omega)$, $\varepsilon = 1/\left(LC\Omega^2\right)$, and $i_j = I_{ext,j}/I_{JC}$ (j =1, 2).

System (4) may be re-expressed as:

$$\begin{aligned} \frac{\mathrm{d}\phi_1}{\mathrm{d}t} &= v_1 \\ \frac{\mathrm{d}v_1}{\mathrm{d}t} &= i_1 - \alpha v_1 - \sin(\phi_1) + \varepsilon(\phi_1 - \phi_2) \\ \frac{\mathrm{d}\phi_2}{\mathrm{d}t} &= v_2 \\ \frac{\mathrm{d}v_2}{\mathrm{d}t} &= i_2 - \alpha v_2 - \sin(\phi_2) + \varepsilon(\phi_2 - \phi_1) \end{aligned} \tag{5}$$

System (5) is dissipative because $\frac{\left(\frac{\partial\phi_1}{\partial t}\right)}{\partial\phi_1} + \frac{\left(\frac{\partial v_1}{\partial t}\right)}{\partial v_1} + \frac{\left(\frac{\partial\phi_2}{\partial t}\right)}{\partial\phi_2} + \frac{\left(\frac{\partial v_2}{\partial t}\right)}{\partial v_2} = -2\alpha < 0$. In order to determine the equilibrium points, System (5) is set equal to zero which gives:

$$v_1^* = 0 \tag{6}$$

$$i_1 - \alpha v_1^* - \sin(\phi_1^*) + \varepsilon(\phi_1^* - \phi_2^*) = 0 \tag{7}$$

$$v_2^* = 0 \tag{8}$$

$$i_2 - \alpha v_2^* - \sin\left(\phi_2^*\right) + \varepsilon\left(\phi_2^* - \phi_1^*\right) = 0 \tag{9}$$

Substituting Eq. (6) in Eq. (7) and Eq. (8) in Eq. (9) yields:

$$i_1 - \sin\left(\phi_1^*\right) + \varepsilon\left(\phi_1^* - \phi_2^*\right) = 0 \tag{10}$$

$$i_2 - \sin\left(\phi_2^*\right) + \varepsilon\left(\phi_2^* - \phi_1^*\right) = 0 \tag{11}$$

Eq. (10) + Eq. (11) yields:

$$i_1 + i_2 - \sin\left(\phi_1^*\right) - \sin\left(\phi_2^*\right) = 0 \tag{12}$$

Since $-1 \leq \sin\left(\phi_{1,2}^*\right) \leq 1$, Eq. (12) can be expressed as:

$$i_1 + i_2 \leq 2.0 \tag{13}$$

Solving Eq. (12) for ϕ_2^* and substituting the result into Eq. (11) yields:

$$i_1 - \sin\left(\phi_1^*\right) + \varepsilon\left[\phi_1^* - \arcsin\left(i_1 + i_2 - \sin\left(\phi_1^*\right)\right)\right] = 0 \tag{14}$$

$$\phi_2^* = \arcsin\left[i_1 + i_2 - \sin\left(\phi_1^*\right)\right] \tag{15}$$

Equilibrium points $E\left(\phi_1^*, 0, \phi_2^*, 0\right)$ of System (5) exist only for $i_1 + i_2 < 2$, and Eq. (14) cannot easily be solved analytically. The NewtonRaphson method is used to solve Eq. (14) in order to find the value of ϕ_1^*. The value of ϕ_2^* is obtained by substituting the value of ϕ_1^* into Eq. (15). The characteristic equation of System (5) evaluated at equilibrium points $E\left(\phi_1^*, 0, \phi_2^*, 0\right)$ is defined by:

$$\begin{aligned} \lambda^4 + 2\alpha\lambda^3 + \left[\alpha^2 - 2\varepsilon + \cos\left(\phi_1^*\right) + \cos\left(\phi_2^*\right)\right]\lambda^2 + \alpha\left[\cos\left(\phi_1^*\right) + \cos\left(\phi_2^*\right) - 2\varepsilon\right]\lambda \\ + \cos\left(\phi_1^*\right)\cos\left(\phi_2^*\right) - \varepsilon\cos\left(\phi_1^*\right) - \varepsilon\cos\left(\phi_2^*\right) = 0 \end{aligned} \tag{16}$$

where, $a_1 = 2\alpha$, $a_2 = \alpha^2 - 2\varepsilon + \cos\left(\phi_1^*\right) + \cos\left(\phi_2^*\right)$, $a_3 = \alpha\left[\cos\left(\phi_1^*\right) + \cos\left(\phi_2^*\right) - 2\varepsilon\right]$, and $a_4 = \cos\left(\phi_1^*\right)\cos\left(\phi_2^*\right) - \varepsilon\cos\left(\phi_1^*\right) - \varepsilon\cos\left(\phi_2^*\right)$. According to the Routh-Hurwitz stability criterion, the real parts of all the roots λ of Eq. (16) are negative if and only if:

$$\begin{aligned} a_1 &> 0 \\ a_3 &> 0 \\ a_4 &> 0 \\ a_1 a_2 a_3 - a_3^2 - a_1^2 a_4 &> 0 \end{aligned} \tag{17}$$

The stability of equilibrium points $E\left(\phi_1^*, 0, \phi_2^*, 0\right)$ depends on the parameters α, ε, i_1, and i_2. For a specific value of the parameter α, the stability analysis of equilibrium points $E\left(\phi_1^*, 0, \phi_2^*, 0\right)$ as a function of the parameters ε, i_1, and i_2 of System (5) is depicted in Figure 2.

It can be noticed from Figure 2 that System (5) has only one equilibrium point $E\left(\phi_1^*, 0, \phi_2^*, 0\right)$. In the left panel of the figure, the only equilibrium point is stable for $\varepsilon < 0.53$ in Figure 2a and Figure 2c and unstable for $\varepsilon \geq 0.53$ in Figure 2a and $\varepsilon \geq 0.33$ in Figure 2c. By varying the current $i = i_1 = i_2$ or i_1, the only equilibrium point is always stable, as shown in the right panel of Figure 2. The change in stability observed occurs at $\varepsilon \approx 0.53$ for Figure 2a and at $\varepsilon \approx 0.33$ for Figure 2c. In the following paragraph, The Hopf bifurcation from the only equilibrium point is discussed, taking ε as the bifurcation parameter.

A bifurcation study was conducted. A Hopf bifurcation regarding ε as the bifurcation parameter is considered in order to have a qualitative idea of the behavior of the equilibrium points $E\left(\phi_1^*, 0, \phi_2^*, 0\right)$. Substituting $\lambda = i\omega$ in Eq. (16) and separating real and imaginary parts yields:

$$\omega^2 = \left[\cos\left(\phi_1^*\right)\cos\left(\phi_2^*\right) - 2\varepsilon\right]/2 \tag{18}$$

$$\varepsilon^2 - \alpha^2\varepsilon + \left[\cos\left(\phi_1^*\right) - \cos\left(\phi_2^*\right)\right]^2/4 + \alpha^2\left[\cos\left(\phi_1^*\right) + \cos\left(\phi_2^*\right)\right]^2/2 = 0 \tag{19}$$

A plot of ω^2 versus ε for the obtained values of ϕ_1^* and ϕ_2^* is depicted in Figure 3.

There exists no Hopf bifurcation in System (5) at the equilibrium point $E\left(\phi_1^*, 0, \phi_2^*, 0\right)$ provided $\varepsilon \geq 0.93$ in Figure 3a or $\varepsilon > 0.73$ in Figure 3b. For $\varepsilon \geq 0.93$ or $\varepsilon \geq 0.73$, it can be seen that $\omega^2 < 0$. Thus, the only equilibrium point $E\left(\phi_1^*, 0, \phi_2^*, 0\right)$ does not undergo Hopf bifurcation. Therefore, System (5) at the equilibrium point $E\left(\phi_1^*, 0, \phi_2^*, 0\right)$ has a saddlenode bifurcation at $\varepsilon \approx 0.53$ in Figure 3a and $\varepsilon \approx 0.33$ in Figure 3b.

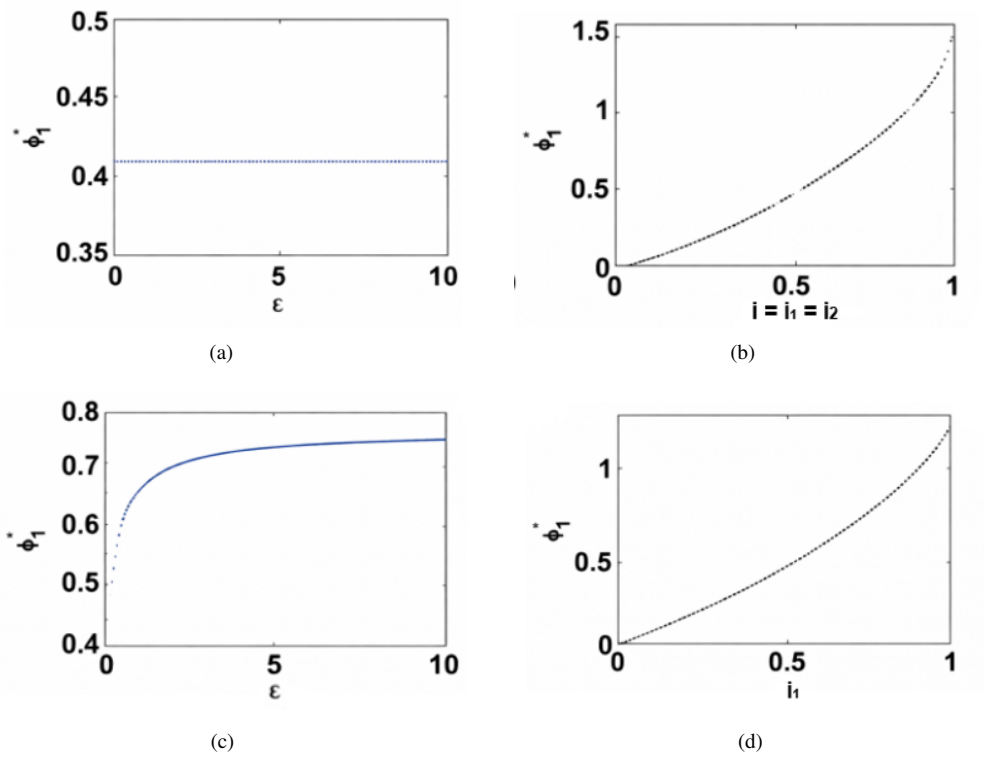

(a) (b)

(c) (d)

Figure 2. Stability diagram of equilibrium points $E\left(\phi_1^*, 0, \phi_2^*, 0\right)$ versus the parameter ε (left panel) and $i = i_1 = i_2$ or i_1 (right panel) for specific values of parameters α, ε, i_1, and i_2: (a) $i_1 = i_2 = 0.4$; (b) $i_1 = 0.4$, $i_2 = 1.0$; (c) $\varepsilon = 0.03291$; and (d) $\varepsilon = 0.03291$, $i_2 = 0.4$

Note: Solid black lines indicate the stable branches and the blue lines indicate the unstable branches. Unless otherwise stated, $\alpha = 0.2$.

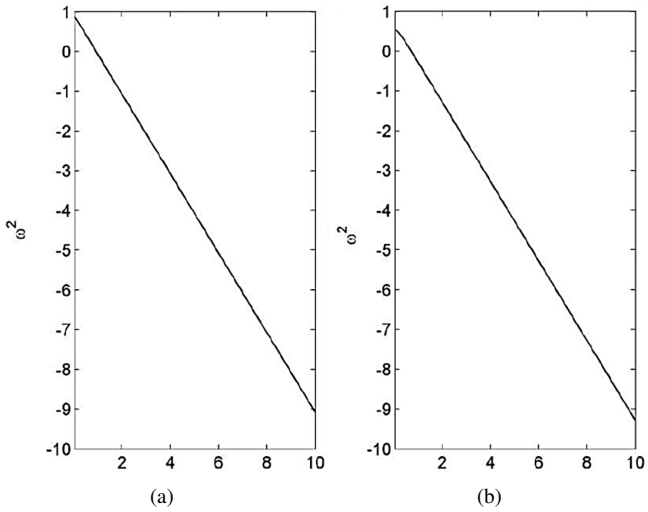

(a) (b)

Figure 3. Parameter ω^2 versus the parameter ε, with ω^2 defined in Eq. (18)

3 Numerical Analysis of Inductively Coupled Direct Current-Driven Identical Linear Resistive-Capacitive Shunted Josephson Junction Circuits

In order to gain more insight into the proposed circuit, it is necessary to study the evolution of the system for specific values of the parameters α and ε and the normalized external DC currents $i_{1,2}$. The dynamical behavior of System (5) can be studied by varying parameter values of ε and $i_{1,2}$ as α is considered to be fixed. Since System (5) has equilibrium points for $i_1 + i_2 \leq 2$ and no equilibrium points for $i_1 + i_2 > 2$, it is interesting to study the dynamical behavior of System (5) for $i_1 + i_2 \leq 2$ and $i_1 + i_2 > 2$. Without the coupling ($\varepsilon = 0.0$), LRCSJJ is said to be in the excitable mode when $i_{1,2} < 1$ and in the oscillatory mode when $i_{1,2} > 1$, as shown in Figure 4.

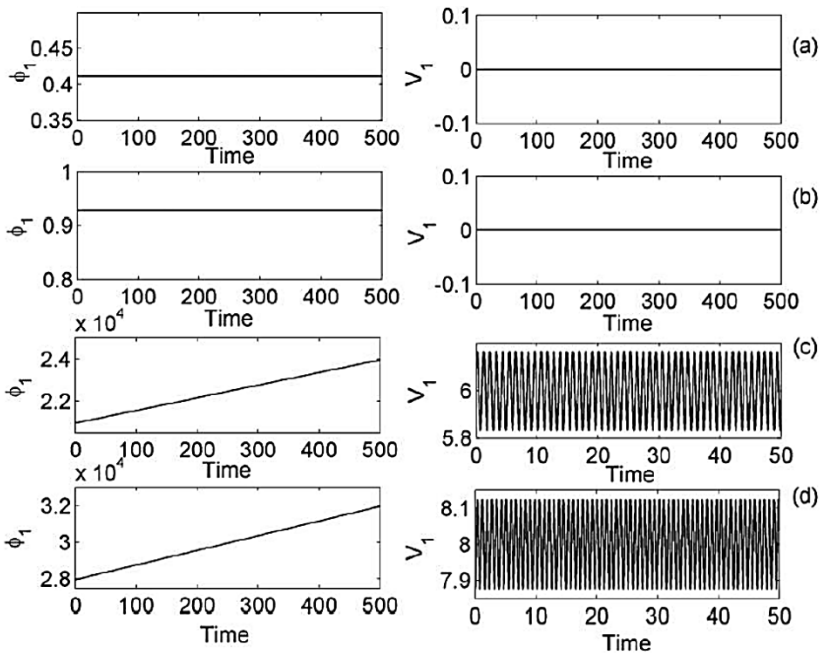

Figure 4. Time series of v_1 and ϕ_1 for specific values of currents: (a) $i_1 = i_2 = 0.4$; (b) $i_1 = i_2 = 0.8$; (c) $i_1 = i_2 = 1.2$; and (d) $i_1 = i_2 = 1.6$. Unless otherwise stated, $\varepsilon = 0.0$ and $\alpha = 0.2$

For $i_1 + i_2 < 2$, the time series of voltages and phases for specific values of normalized external DC sources $i_{1,2}$ are plotted, as shown in Figure 5.

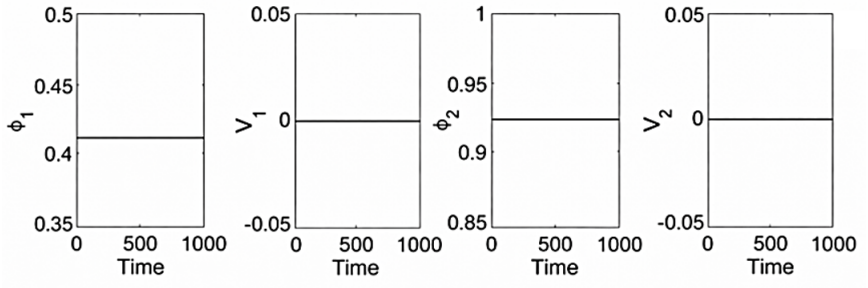

(a)

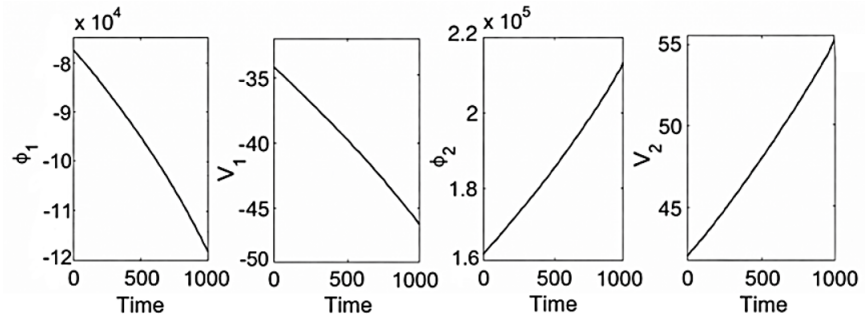

(b)

Figure 5. Time series of $v_{1,2}$ and $\phi_{1,2}$ for specific values of currents: (a) $i_1 = 0.4$ and $i_2 = 0.8$; (b) $i_1 = 0.4$ and $i_2 = 1.2$. Unless otherwise stated, $\varepsilon = 3.0 \times 10^{-5}$ and $\alpha = 0.2$

In Figure 5a, the two LRCSJJ circuits exhibit the excitable mode. In Figure 5b, the trajectories of one JJ decrease exponentially while the trajectories of the other LRCSJJ circuit increase exponentially. For $i_1 + i_2 \geq 2$, the time series of voltages and phases for specific values of normalized external DC sources $i_{1,2}$ are plotted, as shown in Figure 6.

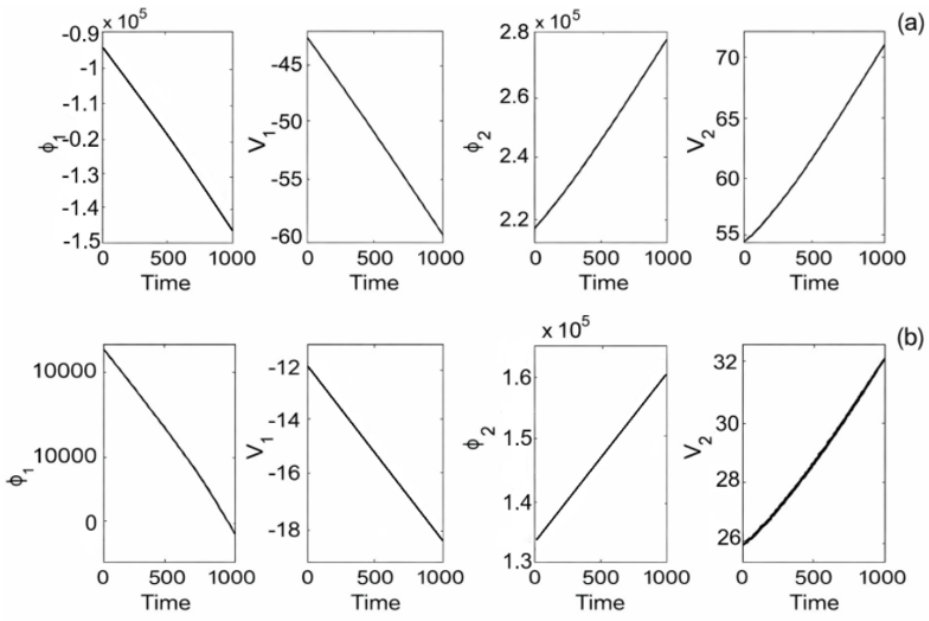

Figure 6. Time series of $v_{1,2}$ and $\phi_{1,2}$ for specific values of currents: (a) i_1 = 0.8 and i_2 = 1.6; (b) i_1 = 1.2 and i_2 = 1.6. Unless otherwise stated, $\varepsilon = 3.0 \times 10^{-5}$ and $\alpha = 0.2$

In Figure 6, the trajectories of one JJ decrease exponentially while the trajectories of the other JJ increase exponentially. A closer observation of the time series in Figure 6 reveals oscillations bounded by the growing curves. Assuming that the normalized external DC currents are equal, i.e., $i_1 = i_2$, the time series of voltages and phases for specific values of normalized external DC sources $i_{1,2}$ are depicted in Figure 7.

In Figure 7, the two JJs exhibit the oscillatory mode. The amplitudes and frequencies of their oscillations increase with the value of the normalized external DC sources.

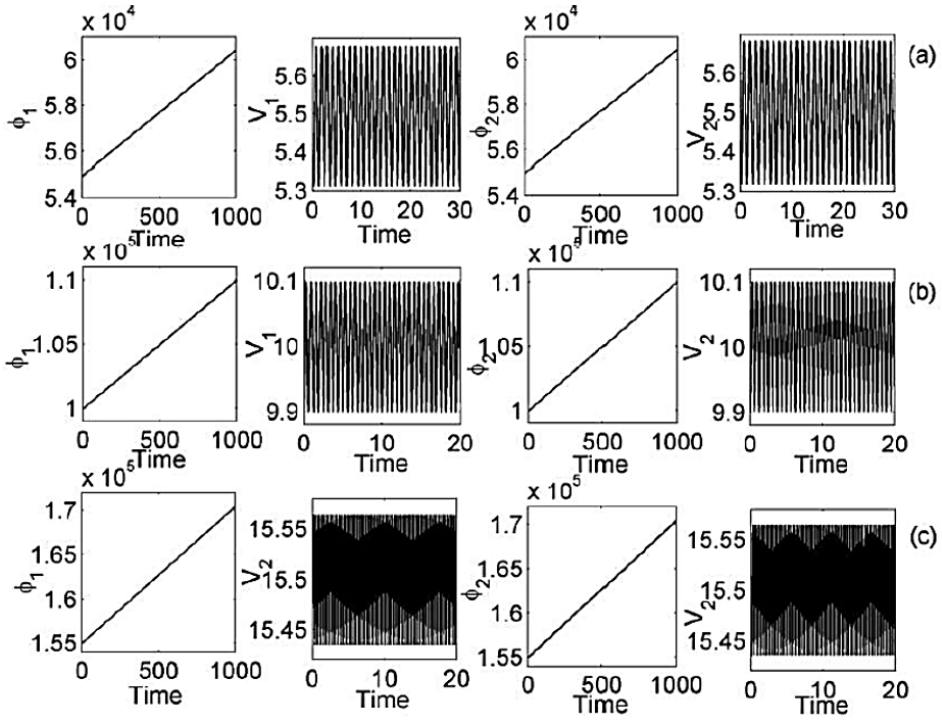

Figure 7. Time series of $v_{1,2}$ and $\phi_{1,2}$ for specific values of currents: (a) $i_1 = i_2$ = 1.1; (b) $i_1 = i_2$ = 2.0; and (c) $i_1 = i_2$ = 3.1. Unless otherwise stated, $\varepsilon = 3.0 \times 10^{-5}$ and $\alpha = 0.2$

4 Conclusion

This study presents the modeling and dynamical analysis of two identical LRCSJJs coupled through an inductor. The governing rate equations of the system were derived by applying Kirchhoff's circuit laws. The analysis revealed that the proposed system possesses a single equilibrium point. By employing the Routh-Hurwitz stability criterion, this equilibrium was shown to remain stable for normalized currents satisfying $i_1 + i_2 \leq 2$ and for coupling strengths $\varepsilon < 0.53$. A further analytical investigation of the equilibrium point demonstrated that a saddle-node bifurcation occurs at approximately $\varepsilon \approx 0.53$. In addition to the analytical results, extensive numerical simulations were performed to explore the system dynamics. For appropriate choices of the coupling parameter and the external DC currents i_1 and i_2, the circuit was found to exhibit both excitable behavior and sustained oscillatory regimes. As a perspective for future work, it would be of particular interest to extend the present analysis to inductively coupled non-identical resistive-capacitive shunted JJ circuits. Such an investigation could reveal the emergence of more complex dynamical phenomena, including chaotic or hyperchaotic behavior.

Author Contributions

Conceptualization, G.K., L.M., and A.S.K.T.; methodology, A.S.K.T., O.A.A., and N.F.F.F.; software, A.S.K.T., L.M., O.A.A., and N.F.F.F.; validation, G.K., L.M., and A.S.K.T.; formal analysis, A.S.K.T., L.M., O.A.A., and N.F.F.F.; investigation, A.S.K.T., L.M., O.A.A., and N.F.F.F.; resources, A.S.K.T., L.M., O.A.A., and N.F.F.F.; data curation, A.S.K.T., L. M., O.A.A., and N.F.F.F.; writing—original draft preparation, L.M. and A.S.K.T.; writing—review and editing, L.M. and A.S.K.T.; visualization, G.K.; supervision, G.K. All authors have read and agreed to the published version of the manuscript.

Data Availability

The data used to support the research findings are available from the corresponding author upon request.

Conflicts of Interest

The authors declare no conflicts of interest.

References

[1] B. D. Josephson, "Possible new effects in superconductive tunnelling," *Phys. Lett.*, vol. 1, no. 7, pp. 251–253, 1962. https://doi.org/10.1016/0031-9163(62)91369-0

[2] B. Soodchomshom, I. M. Tang, and R. Hoonsawat, "Josephson effects in MgB_2/thin insulator/MgB_2 tunnel junction," *Solid State Commun.*, vol. 149, no. 25-26, pp. 1012–1016, 2009. https://doi.org/10.1016/j.ssc.2009.04.007

[3] J. Clarke, "A superconducting galvanometer employing Josephson tunnelling," *Philos. Mag.*, vol. 13, no. 121, pp. 115–127, 1966. https://doi.org/10.1080/14786436608211991

[4] A. B. Cawthorne, P. Barbara, S. V. Shitov, C. J. Lobb, K. Wiesenfeld, and A. Zangwill, "Synchronized oscillations in Josephson junction arrays: The role of distributed coupling," *Phys. Rev. B*, vol. 60, no. 10, p. 7575, 1999. https://doi.org/10.1103/PhysRevB.60.7575

[5] C. B. Whan, C. J. Lobb, and M. G. Forrester, "Effect of inductance in externally shunted Josephson tunnel junctions," *J. Appl. Phys.*, vol. 77, no. 1, pp. 382–389, 1995. https://doi.org/10.1063/1.359334

[6] C. B. Whan and C. J. Lobb, "Complex dynamical behavior in RCL-shunted Josephson tunnel junctions," *Phys. Rev. E*, vol. 53, no. 1, p. 405, 1996. https://doi.org/10.1103/PhysRevE.53.405

[7] S. T. Kingni, G. Fautso Kuiate, R. Kengne, R. Tchitnga, and P. Woafo, "Analysis of a no equilibrium linear resistive-capacitive-inductance shunted junction model, dynamics, synchronization, and application to digital cryptography in its fractional-order form," *Complexity*, vol. 2017, no. 1, p. 4107358, 2017. https://doi.org/10.1155/2017/4107358

[8] J. Clarke and A. I. Braginski, *The SQUID Handbook: Fundamentals and Technology of SQUIDs and SQUID Systems*. John Wiley & Sons, 2006.

[9] W. C. Stewart, "Current-voltage characteristics of Josephson junctions," *Appl. Phys. Lett.*, vol. 12, no. 8, pp. 277–280, 1968.

[10] D. E. McCumber, "Effect of AC impedance on DC voltage-current characteristics of superconductor weak-link junctions," *J. Appl. Phys.*, vol. 39, no. 7, pp. 3113–3118, 1968. https://doi.org/10.1063/1.1656743

[11] M. Levi, F. C. Hoppensteadt, and W. L. Miranker, "Dynamics of the Josephson junction," *Quart. Appl. Math.*, vol. 36, no. 2, pp. 167–198, 1978. https://doi.org/10.1090/qam/484023

[12] F. Salam and S. Sastry, "Dynamics of the forced Josephson junction circuit: The regions of chaos," *IEEE Trans. Circuits Syst.*, vol. 32, no. 8, pp. 784–796, 2003. https://doi.org/10.1109/TCS.1985.1085790

[13] E. Kurt and M. Canturk, "Chaotic dynamics of resistively coupled DC-driven distinct Josephson junctions and the effects of circuit parameters," *Physica D*, vol. 238, no. 22, pp. 2229–2237, 2009. https://doi.org/10.1016/j.physd.2009.09.005

[14] B. Nana, P. Woafo, and S. Domngang, "Chaotic synchronization with experimental application to secure communications," *Commun. Nonlinear Sci. Numer. Simul.*, vol. 14, no. 5, pp. 2266–2276, 2009. https://doi.org/10.1016/j.cnsns.2008.06.028

[15] S. T. Kingni, Hervé Talla Mbé, J., and P. Woafo, "Semiconductor lasers driven by self-sustained chaotic electronic oscillators and applications to optical chaos cryptography," *Chaos*, vol. 22, no. 3, 2012. https://doi.org/10.1063/1.4733702

[16] S. T. Kingni, "Dynamics and synchronisation of VCELs and SRLs subject to current modulation and optical/optoelectronic feedback," Ph.D. dissertation, Vrije Universiteit Brussel, 2014.

[17] M. A. H. Nerenberg, J. A. Blackburn, and D. W. Jillie, "Voltage locking and other interactions in coupled superconducting weak links. I. Theory," *Phys. Rev. B*, vol. 21, no. 1, p. 118, 1980. https://doi.org/10.1103/PhysRevB.21.118

[18] M. A. H. Nerenberg, J. A. Blackburn, and S. Vik, "Chaotic behavior in coupled superconducting weak links," *Phys. Rev. B*, vol. 30, no. 9, p. 5084, 1984. https://doi.org/10.1103/PhysRevB.30.5084

[19] D. Dominguez and H. A. Cerdeira, "Order and turbulence in rf-driven Josephson junction series arrays," *Phys. Rev. Lett.*, vol. 71, no. 20, p. 3359, 1993. https://doi.org/10.1103/PhysRevLett.71.3359

[20] B. P. Koch and B. Bruhn, "Transient chaos in weakly coupled Josephson junctions," *J. Phys.*, vol. 49, no. 1, pp. 35–40, 1988. https://doi.org/10.1051/jphys:0198800490103500

[21] C. R. Nayak and V. C. Kuriakose, "Dynamics of coupled Josephson junctions under the influence of applied fields," *Phys. Lett. A*, vol. 365, no. 4, pp. 284–289, 2007. https://doi.org/10.1016/j.physleta.2007.01.018

[22] E. Kurt and M. Canturk, "Bifurcations and hyperchaos from a DC driven nonidentical Josephson junction system," *Int. J. Bifurc. Chaos*, vol. 20, no. 11, pp. 3725–3740, 2010. https://doi.org/10.1142/S021812741002801X

[23] T. Hongray, J. Balakrishnan, and S. K. Dana, "Bursting behaviour in coupled Josephson junctions," *Chaos*, vol. 25, no. 12, p. 123104, 2015. https://doi.org/10.1063/1.4936675

[24] M. Agaoglou, V. M. Rothos, and H. Susanto, "Homoclinic chaos in coupled SQUIDs," *Chaos Solitons Fractals*, vol. 99, pp. 133–140, 2017. https://doi.org/10.1016/j.chaos.2017.04.003

[25] D. T. Ngatcha, B. P. Ndemanou, A. F. Talla, S. G. N. Mbouna, and S. T. Kingni, "Numerical exploration of a network of nonlocally coupled Josephson junction spurred by Wien Bridge Oscillators," *Chaos and Fractals*, vol. 1, no. 1, pp. 1–5, 2024. https://doi.org/10.69882/adba.chf.2024071

[26] J. Metsebo, B. Abdou, D. T. Ngatcha, I. K. Ngongiah, P. D. K. Kuate, and J. R. M. Pone, "Analysis of a resistive-capacitive shunted Josephson junction with topologically nontrivial barrier coupled to a RLC resonator," *Chaos and Fractals*, vol. 1, no. 1, pp. 31–37, 2024. https://doi.org/10.69882/adba.chf.2024074